MACSima™ Imaging Platform provides new insights into cancer biology and target discovery by cyclic immunofluorescence–based imaging

Christoph Herbel, Sandy Reiß, Melanie Jungblut, Dominik Eckardt, and Andreas Bosio on behalf of the MACSima Team* and Target Discovery Team*
Miltenyi Biotec GmbH, Bergisch Gladbach, Germany

* Team members in alphabetical order: Ali Kinkhabwala, Bastian Ackermann, Eik Schumann, Jan Drewes, Jan Keseberg, Joachim Bächle, Jürgen Krieg, Jürgen Schmitz, Jutta Kollett, Manuel Martinez-Osuna, Nadine Küster, Olaf Hardt, Ralf-Peter Peters, Silvia Rüberg, Stefan Borbe, Stefan Eulitz, Stefan Miltenyi, Stefan Tomiuk, Vera Dittmer, Volker Lutter, Werner Müller, and Yvonne Dürnberger

Analysis of cancer cell diversity and immune contexture based on protein expression is of high relevance for tumor subclassification and the development of novel targeted immunotherapies. However, these kinds of analyses are currently hampered by the lack of technologies that allow for sensitive and comprehensive multiplexed protein analysis. The novel MACSima™ Imaging Platform enables high-content, cyclic fluorescence–based imaging of individual biological samples in a fully automated fashion. We demonstrate how this novel platform can be used to analyze, for example, ovarian tumor and glioblastoma samples in research towards the discovery of potential targets for immunotherapy.

MACSima™ Imaging Platform – breaking the limits of antibody multiplexing in microscopy

Microscopy has made major progress in the last decades towards higher resolution, sensitivity, and tissue penetration, in particular by two-photon and light sheet microscopy. A further demand has been to increase the number of detectable targets on a single specimen. In standard fluorescent microscopy, multiplexing is restricted due to the range of excitation and emission spectra of fluorescent dyes and the limited spectrum of visible light. Increasing the number of dyes imaged simultaneously, ultimately leads to an overlap of spectra which – depending on the resolution – cannot be properly compensated. Therefore, many new technologies, either using optical or mass spectrometric readouts, have been introduced, including multi-epitope-ligand cartography (MELC)[1], ChipCytometry[2,3], mass cytometry[4], multiplexed ion beam imaging (MIBI)[5], cyclic immunofluorescence (CycIF)[6], multiplex immunohistochemistry[7], co-detection by indexing (CODEX)[8], Digital Spatial Profiling (NanoString®, NanoString Technologies Inc.), or InSituPlex® Technology (Ultivue Inc.).

Based on the MELC technology we have developed a new imaging platform for cyclic immunofluorescence analysis, introducing innovative solutions to address a number of shortcomings experienced with other technologies. The MACSima™ Imaging Platform provides a complete, integrated system including instrument (fig. 1A), optimized sample carriers, validated antibodies, and software. It operates by iterative fluorescent staining, image acquisition, and signal erasure, using multiple fluorochrome-conjugated antibodies per cycle (fig. 1B). Cyclic processing allows for the analysis of hundreds of different markers on a single sample.

The MACSima Imaging System includes optics (epifluorescence microscope, sCMOS camera, five emission filters, autofocus, six LEDs, three lenses), fluidics, mechanics (100 nm stage resolution), and data storage. The system allows fully automated processing of eight microscope slides or two 24-well imaging plates with hundreds of fluorochrome-conjugated antibodies or antibody fragments in a single run. Specially developed sample carriers, the MACSwell Imaging Frames, provide one, two, or four cavities and are mounted on standard microscope slides. MACSwell Micro Slides contain hundreds of thousands of small cavities that exactly fit one cell. Based on these sample carriers the system can process solid tissue slices, adherent cells, and suspension cells.

Two types of proprietary conjugates have been qualified for the analysis on the MASCima Imaging System: fluorochrome-conjugated REAfinity™ Recombinant Antibodies and REAlease® Releasable Antibodies. REAfinity Antibodies provide a higher lot-to-lot consistency and purity compared to mouse or rat hybridoma-derived monoclonal antibodies. All REAfinity Antibodies are recombinantly engineered using the same IgG1 isotype backbone. They do not require any FcR blocking step and thus are highly specific. REAlease Releasable Antibodies are a new type of antibody-fluorochrome conjugates, generated based on recombinantly engineered antibody fragments that individually possess low epitope binding affinities. A novel conjugation approach enables multimerization and fluorescent labeling of the fragments. The resulting complex can then bind to cell surface epitopes with high avidity. Subsequent disruption of the complex leads to release of the conjugates from the cell.

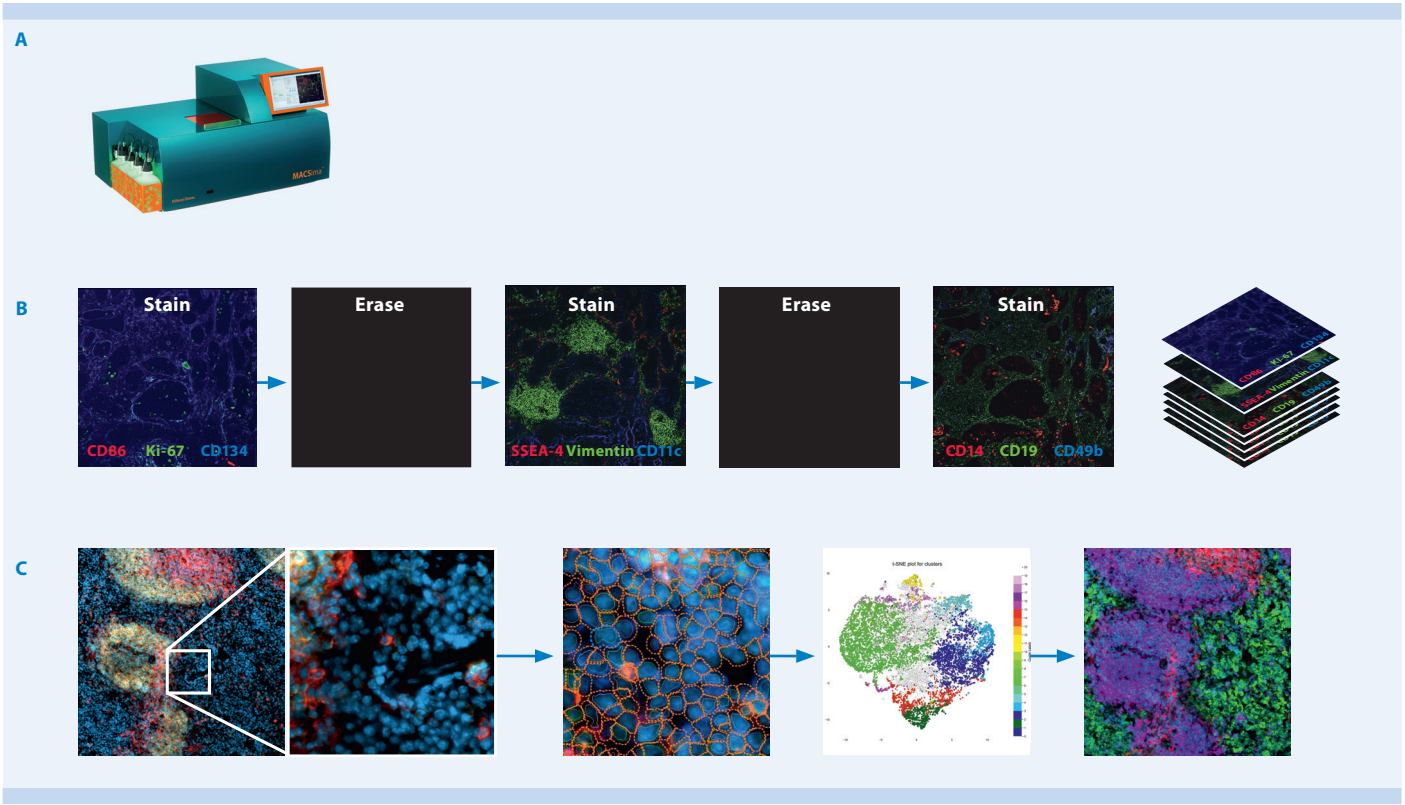

Figure 1: MACSima System enables high-content imaging. A cyclic process consisting of sample staining, image acquisition, and signal erasure is performed fully automatically by the MACSima Imaging System (A) and results in stacks of potentially hundreds of images (B). After segmentation of the image, multiple clustering methods can be visualized as scatter diagrams and back-plotted onto the initial image (C).

A plethora of REAfinity™ and REAlease® Antibodies coupled to FITC, PE, and APC are already available for use in combination with the MACSima™ Imaging System. Various antibody plates (REAscreen), each including hundreds of antibodies, were compiled for the analysis of acetone- or paraformaldehyde (PFA)-fixed or formaldehyde-fixed paraffin-embedded (FFPE) samples from human or mouse.

Finally, in-depth analysis of the image stacks generated on the instrument is achieved using a software developed in collaboration with Quantitative Imaging Systems. It allows an easy navigation through the hundreds of images and helps to identify markers and cell types of interest by segmenting images into single cells and clustering cells and proteins according to their profile across all cells. Multiple different clustering methods can be applied and visualized as scatter diagrams or back-plotted onto the microscopic image (fig. 1C).

Comprehensive cyclic immunofluorescence analysis reveals new target candidates for chimeric antigen receptor–expressing T cells

The advent of chimeric antigen receptor (CAR) T cell technology has opened new perspectives in the fight against cancer. CAR T cell–based therapies have resulted in a remarkable success in the treatment of hematopoietic malignancies[9,10], but have not yet led to a breakthrough in eliminating solid tumors. Besides numerous tissue-immanent obstacles hampering T cell infiltration, such as the tumor microenvironment, part of the problem is also the lack of proteins that are suitable as targets for CAR T cells.

When considering a protein as a target for immunotherapy the coverage of tumor cells is predictive for its efficacy while the on-target/off-tumor toxicity is a potential threat. On-target/off-tumor toxicity is mainly based on the expression of tumor-associated antigens in healthy tissues under physiological conditions. Currently, most prediction methods for on-target/off-tumor expression are based on single-cell or even bulk mRNA expression data on healthy tissue. These models, however, have limitations, mainly due to poor predictability of the correlation between RNA and protein levels.

A number of cell surface markers are currently being investigated in CAR T cell therapy for solid tumors such as mesothelin (MSLN), ErbB2 (HER2), EGFR/EGFRvIII, GD2, CEA, IL-13Rα2, MUC1, FAP, PSMA, and PSCA.[11]

We have used the MACSima Imaging Platform to analyze the toxicity profile of some of these markers and to screen for alternative markers. To that end, we analyzed a variety of tumor samples including glioblastoma, ovarian and pancreatic cancer and re-assessed potential markers for their expression profile in healthy tissue. Two studies exemplifying the power of the technology are discussed below.

Evaluation of the specificity and tissue distribution of MUC1

MUC1 (also termed mucin-1, a transmembrane glycoprotein) is an example of a marker which is aberrantly up-regulated in many types of cancer and is under evaluation in clinical trials as target for CAR T cells.[11] It is also well established that mucins line the apical surface of epithelial cells in the lungs, stomach, intestines, eyes, and several other organs.[12] To better understand the uniformity of MUC1 expression on tumor cells, we analyzed several patient-derived high-grade serous ovarian carcinomas using the MACSima™ Imaging Platform. Figure 2 shows a subset of the multiparameter expression analysis of MUC1 and markers indicative of cell lineages and proliferation status, i.e., CD326 (epithelial), Ki-67 (proliferation), CD31 (endothelial), CD90 (stromal), and CD45 (differentiated hematopoietic cells). MUC1 was expressed on all analyzed ovarian carcinoma samples and, based on the co-expression with CD326 (EpCAM), it could be assigned to epithelial cells. This corroborates previous reports[13] and suggests MUC1 as a potential target. However, the percentage of MUC1-positive cells among the different samples was highly variable. Moreover, MUC1 did not cover the complete population of CD326-positive cells in these tumors, which questions the selectivity of MUC1 as a CAR T cell target. Similar results were obtained for pancreatic ductal adenocarcinoma (not shown).

Next, we assessed the expression of MUC1 in healthy human tissues, i.e., kidney, colon, heart, lung, skin, and breast. As shown in figure 3, analysis of MUC1 compared to different lineage markers, i.e., CD326 (epithelial), CD29 (diverse), vimentin (mesenchymal), CD105 (endothelial, stromal), and CD90 (stromal) revealed that MUC1 was expressed on epithelial cells in different healthy human tissues. This finding not only stresses the importance of pre-clinical target validation on healthy tissues to predict potential on-target/off-tumor toxicity but also indicates which tissues and cell types could be affected when using MUC1 as target in CAR T cell therapies.

Characterization and classification of glioblastoma multiforme for the identification of new glioblastoma-specific markers

Glioblastoma multiforme is a highly malignant, incurable type of brain tumor. Current standard-of-care includes radiation, chemotherapy, and surgical resection when possible. Despite advances in each of these treatment modalities, survival rates for pediatric and adult high-grade glioma patients has remained largely unchanged over the course of several years.[14]

To identify new glioblastoma markers, we performed a two-step screening approach. First, patient-derived glioblastoma xenografts were dissociated into single cells using the Tumor Dissociation Kit, human and the gentleMACS™ Octo Dissociator with Heaters. The Mouse Cell Depletion Kit was applied to remove contaminating mouse cells and to obtain a pure xenograft cell suspension. Cells were analyzed by flow cytometry for cell surface marker expression using 523 fluorochrome-conjugated antibodies (MACS® Marker Screen, human and additional 152 antibodies).

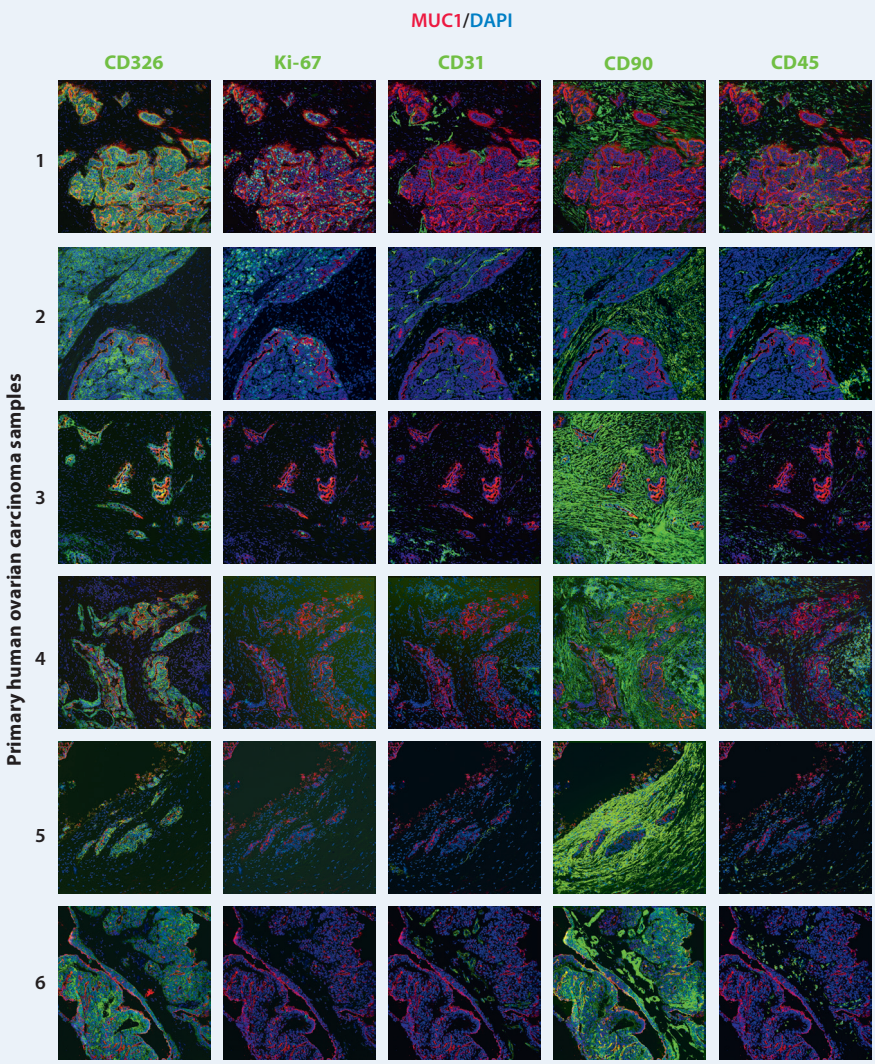

Figure 2: MUC1 shows epithelial expression as well as inter- and intratumor heterogeneity. Multiparameter immunofluorescence-based imaging of six patient-derived high-grade serous ovarian carcinoma samples was performed on the MACSima Imaging System to assess co-expression of MUC1 with different lineage markers, i.e., CD326, Ki-67, CD31, CD90, and CD45. MUC1 is shown in red, DAPI in blue, and the indicated markers in green.

A ranking was applied according to the percentage of positive cells and the stain index, leading to a selection of 96 markers. In a second step, these markers were used for immunohistochemical characterization of primary glioblastoma samples using the MACSima™ Imaging System. To this end, fresh frozen cryosections of different glioblastomas were fixed with acetone. Each specimen was exposed to 96 fluorescently labeled antibodies by repeated cycles of antibody staining, image acquisition of each region of interest (ROI), and erasure of the fluorescence signal. The resulting 2D image stacks were segmented and single-cell imaging data were used for protein expression profiling and pattern recognition.

We classified the different primary glioblastoma tumors based on the expression of PDGFRα, p53, synaptophysin, CD44, nestin, podoplanin, GFAP, and EGFR and following a classification scheme published by Motomura *et al.*[15]

Figure 4 shows representative immunofluorescence stainings of two glioblastoma samples and their classification as either mixed type (fig. 4A), characterized amongst others by a high expression of EGFR, or as astrocytic/mesenchymal type (fig. 4B), which is characterized by strong expression of GFAP, podoplanin, CD44, and nestin, moderate expression of p53 and PDGFRα and is negative for EGFR.

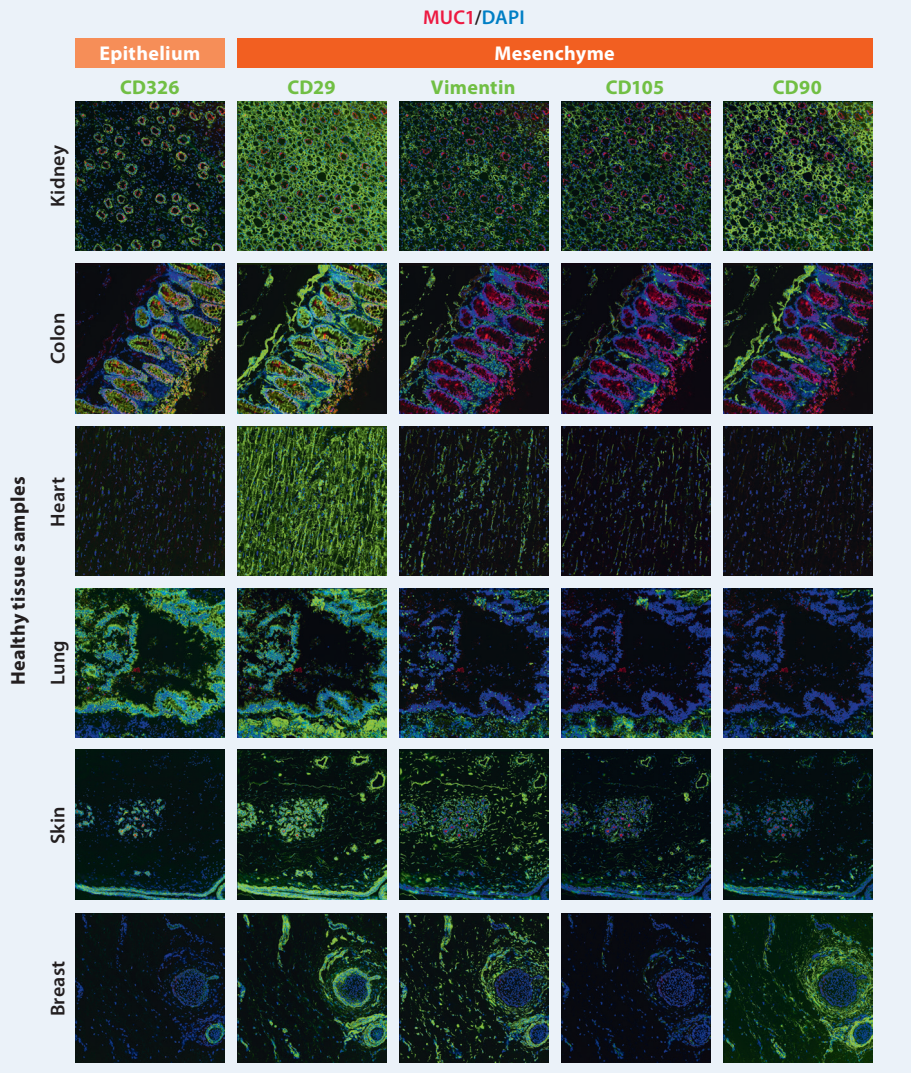

Figure 3: MUC1 is expressed in epithelium of healthy human tissues. Multiparameter immunofluorescence-based imaging of healthy human kidney, colon, heart, lung, skin, and breast tissue was performed using the MACSima Imaging System to assess co-expression of MUC1 with different lineage markers, i.e., CD326, CD29, vimentin, CD105, and CD90. MUC1 is shown in red, DAPI in blue, and the indicated markers in green.

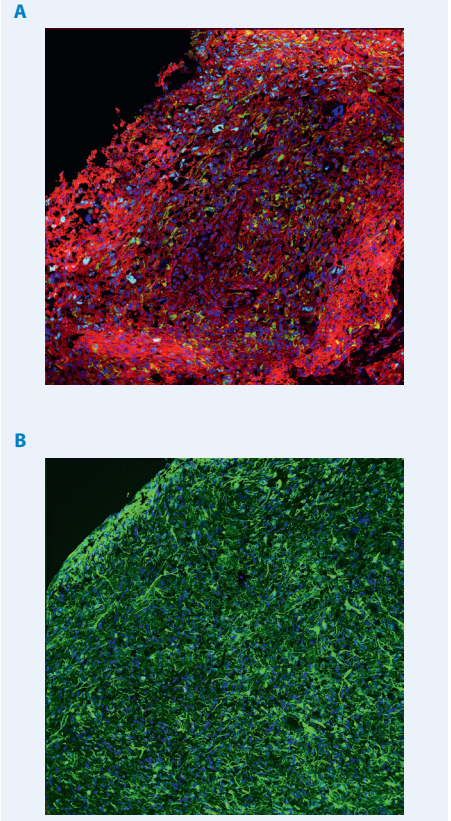

Figure 4: Classification of primary glioblastoma tumors. Immunofluorescence-based imaging was performed using the MACSima Imaging System. Representative immunohistochemical stainings of two glioblastoma samples are shown. According to the classification by Motomura *et al.*[15] the sample shown in (A) is classified as mixed type due to high expression levels of EGFR. In contrast, the sample in (B) belongs to the astrocytic/mesenchymal type, which is characterized by strong expression of GFAP, podoplanin, CD44, and nestin, moderate expression of p53 and PDGFRα, and is negative for EGFR. EGFR is shown in red, nestin in green, p53 in cyan, and DAPI in blue.

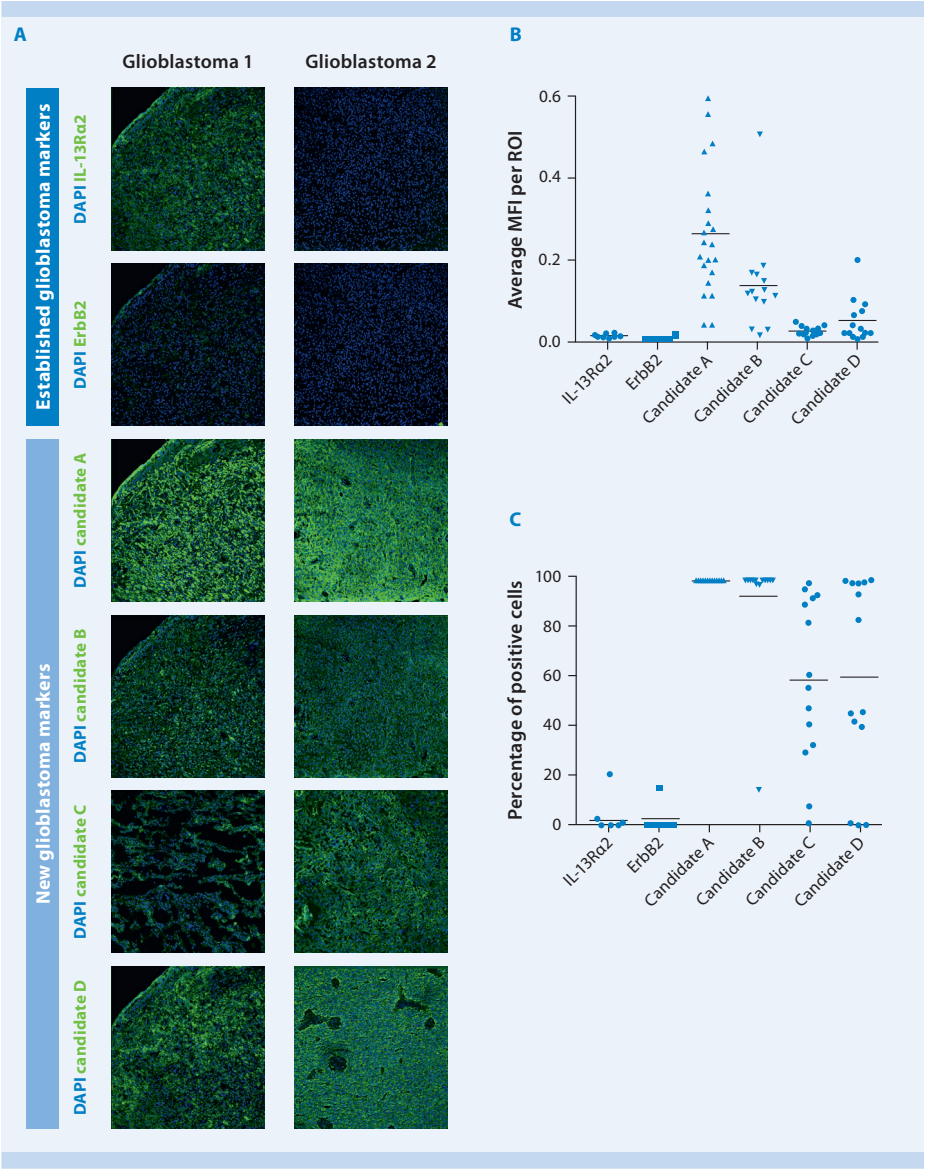

Figure 5: Identification of new glioblastoma-specific markers. Glioblastoma specimens were analyzed using the MACSima™ Imaging System with regard to the expression of well-established glioblastoma markers, i.e., ErbB2, and IL-13Rα2 (A). Screening of 96 antibodies led to the identification of new marker candidates (A). Graphs show average mean fluorescence intensities (MFI) per region of interest (ROI) of the known glioblastoma markers and the new marker candidates (B), and the percentage of positive cells, i.e., cells per ROI with an MFI above background (C). Lines indicate mean values.

Next, we analyzed the expression of well-established glioblastoma markers used in CAR T cell–based clinical trials, such as ErbB2 (HER2) and IL-13Rα2. Our multiparametric cyclic immunofluorescence data indicated only restricted expression of ErbB2 and IL-13Rα2 in these tumors (fig. 5A). However, quantification of single-cell signal intensities of all 96 applied antibodies revealed potential new markers. Compared to known glioblastoma markers, the new marker candidates showed higher expression levels and percentages of positive cells. Figure 5B displays the average mean fluorescence intensity (MFI) per region of interest (ROI), and figure 5C the percentage of cells per ROI with an MFI above background. As a next step, expression of these marker candidates on healthy tissue will be analyzed before generating and testing the corresponding CAR T cells.

Conclusion and outlook

In summary, we introduce a novel, fully integrated and automated cyclic immunofluorescence imaging platform that can be used to analyze a broad variety of specimens with an unprecedented number of antibodies. This technology, which is tailored to maximize the information obtainable from valuable tumor biopsy material, opens up new perspectives for understanding the complexity of tumors and will have a deep impact on the study of tumor stratification and the development of new therapies. Integration of the single-cell protein profiles derived from this technology with single-cell sequencing and 3D microscopy data will be the next steps to expand our knowledge on healthy and diseased cells even further.

References

1. Schubert, W. *et al.* (2006) Nat. Biotechnol. 24: 1270–1278.
2. Perreau, V. M. *et al.* (2010) Proteomics 10: 2377–2395.
3. Hennig, C. *et al.* (2009) Cytometry A 75: 362–370.
4. Bendall, S. C. *et al.* (2011) Science 332: 687–696.
5. Rimm, D. L. (2014) Nat. Methods 11: 381–383.
6. Lin, J. R. *et al.* (2015) Nat. Commun. 6: 8390.
7. Tsujikawa, T. *et al.* (2017) Cell Rep. 19: 203–217.
8. Goltsev, Y. *et al.* (2018) Cell 174: 968–981.
9. Maude, S. L. *et al.* (2018) N. Engl. J. Med. 378: 439–448.
10. Neelapu, S. S. *et al.* (2017) N. Engl. J. Med. 377: 2531–2544.
11. Li, J. *et al.* (2018) J. Hematol. Oncol. 11: 22.
12. Hollingsworth, M. A. and Swanson, B. J. (2004) Nat. Rev. Cancer 4: 45–60.
13. Thie, H. *et al.* (2011) PLoS One 6: e15921.
14. Petersen, C. T. and Krenciute, G. (2019) Front. Oncol. 9: 69.
15. Motomura, K. *et al.* (2012) Cancer Sci. 103: 1871–1879.

Acknowledgments

Tissue samples were kindly provided by Philipp Ströbel (University Medical Center Göttingen, Institute of Pathology, Göttingen, Germany), Wolfgang Brück (University Medical Center Göttingen, Institute of Neuropathology, Göttingen, Germany), Peter Mallmann, Michael Mallmann, and Dominik Ratiu (University of Cologne, Department of Obstetrics and Gynecology, Medical Faculty, Cologne, Germany).